



Investigation of Flap Dimensional Parameters to Improve Hydrodynamic Performance of Oscillating Wave Surge Converter Device

Investigasi Parameter Dimensi Flap Guna Meningkatkan Kinerja Hidrodinamika Perangkat Oscillating Wave Surge Converter

Rizki Aldi Anggara¹, James Julian^{1*}, Fitri Wahyuni¹, Riki Hendra Purba¹, Nely Toding Bunga²

¹Department of Mechanical Engineering, Faculty of Engineering, Universitas Pembangunan Nasional Veteran Jakarta, Jawa Barat, Indonesia

²Department of Mechanical Engineering, Faculty of Engineering, Universitas Pancasila, Jakarta, Indonesia

Article information:

Received:
09/12/2024
Revised:
18/12/2024
Accepted:
19/12/2024

Abstract

Renewable energy transition is a strategic step in overcoming environmental damage due to fossil fuel exploitation. Ocean wave energy comes with its popularity, considering its advantages in supplying energy continuously and having high energy density. Therefore, technology that can extract other wave energy effectively and efficiently is needed. This study focuses on identification flap geometry to improve the oscillating wave surge converter (OWSC) hydrodynamic performance. Through a numerical approach, the Boundary Element Method (BEM) is applied in three-dimensional flap modeling to accommodate testing the characteristics and performance of the OWSC device. This study investigated five different samples: geometry 1, geometry 2, geometry 3, geometry 4, and geometry 5. The results show that the second geometry variation is the most optimal flap dimension parameter. The best proportion is found in the dimensional characteristics parallel to the elevation of the ocean waves to maximize the output torque. Overall, the second geometry performs satisfactorily with an average maximum power achievement of 41.52 Watts at a wave period of $T = 1.5s$. In addition, the OWSC device with this variation can work at an expansive wave period interval with a maximum CWR efficiency achievement of up to 52.14%.

Keywords: BEM, energy, efficiency, hydrodynamic, OWSC.

SDGs:



Abstrak

Transisi energi terbarukan merupakan langkah strategis dalam menganggulangi kerusakan lingkungan akibat eksploitasi energi fosil. Energi gelombang laut hadir dengan popularitasnya mengingat kelebihannya dalam mensuplai energi secara terus menerus dan memiliki kepadatan energi yang tinggi. Oleh karena itu, diperlukan sebuah teknologi yang mampu mengekstrak energi gelombang lain dengan efektif dan efisien. Penelitian ini berfokus pada investigasi geometri flap guna meningkatkan performa hidrodinamika perangkat *Oscillating Wave Surge Converter* (OWSC). Melalui pendekatan numerik, *Boundary Element Method* (BEM) diterapkan dalam pemodelan tiga dimensi flap untuk mengakomodasi pengujian karakteristik dan performa perangkat OWSC. Penelitian ini menginvestigasi lima sampel yang meliputi; geometri 1, geometri 2, geometri 3, geometri 4, dan geometri 5. Hasil penelitian menunjukkan bahwa variasi geometri 2 terbukti merupakan parameter dimensi flap yang paling optimal. Proporsi yang optimal ditemukan pada karakteristik dimensi yang sejajar dengan elevasi gelombang laut sehingga memaksimalkan torsi output. Secara keseluruhan, geometri dua menunjukkan kinerja yang memuaskan dengan capaian rata-rata power maksimum hingga 41.52 Watt di periode gelombang $T = 1.5s$. Selain itu, kapabilitas perangkat OWSC dengan variasi ini mampu bekerja pada interval periode gelombang yang luas dengan capaian efisiensi CWR maksimum hingga 52.14%.

Kata Kunci: BEM, energi, efisiensi, hidrodinamika, OWSC.

*Correspondence Author
email : james@upnvj.ac.id



This work is licensed under a [Creative Commons Attribution-NonCommercial 4.0 International License](https://creativecommons.org/licenses/by-nc/4.0/)

1. INTRODUCTION

Exploitation of oil, gas, and coal as the primary energy sources has raised global concerns about potential impacts (Khaligh and Onar, 2017; Junejo, Saeed and Hameed, 2018; Kadu, Rathod and Matre, 2019). Immediate action is needed to address dependence on environmentally unfriendly energy to prevent environmental damage, air pollution, and long-term conflicts in the next few decades (Sugianto *et al.*, 2017). Renewable energy as an alternative energy transition is a priority for every country in developing national energy security regulations. Ocean wave energy is becoming more widespread as a source of renewable energy due to its benefits, such as continuous energy supply and high energy density (Li *et al.*, 2022). Consequently, it is imperative to develop devices that exploit ocean wave energy to improve the effectiveness and maximization of sustainable energy utilization efforts.

The oscillating wave surge converter (OWSC) is one of the wave energy converters (WEC) types that has garnered significant attention from researchers. It is believed to have the potential to generate more annual power than other WEC devices (Babarit *et al.*, 2012). This device has a track record of achieving promising technological breakthroughs. A notable instance of innovation facilitated by this technology is the development of the Oyster 800. This full-scale prototype, conceived by Aquamarine Power, has undergone rigorous testing and has successfully integrated electrical energy into the national grid since 2011 (O'Boyle *et al.*, 2015). This breakthrough provides an expansive opportunity for researchers to explore OWSC technology innovations. Hydrodynamic studies are one of the essential research activities in the development of OWSC technology. Various studies have focused on developing OWSC devices to improve hydrodynamic performance and efficiency in power plants. Various studies have identified that load damping, geometry, resonant phenomenon, and flap configuration are crucial parameters in determining the hydrodynamic performance of the device (Haitao, 2012; Zhang *et al.*, 2013; Yu *et al.*, 2014; Liu and Zhang, 2024; Munoz, Huang

and Thomas, 2024). Specifically, research focuses on the design and analysis of floating-type OWSC devices with different configuration schematics (Yu *et al.*, 2014). The study revealed that each configuration design is essential in considering the balance of device performance and manufacturing costs. However, some limitations, such as the effect of non-linearity in modeling and secondary estimation data to evaluate the strategy, are minimal. Therefore, it is imperative to exhibit a greater degree of representativeness towards specific domains. In addition, other studies modify the power take-off (PTO) parameters as a resonant adjustment in improving the hydrodynamic performance of OWSC (Liu *et al.*, 2022). Several supporting variables, including damping, stiffness, and PTO inertia, are controlled to meet the resonance phenomenon on the flap and increase the optimal capture width ratio (CWR). In addition, other studies examine dual OWSC followed by variations in the shape of the cross-section on the flap with a numerical approach (Cui, Chen and Dai, 2023). Single OWSC is evaluated as a performance comparison for each different cross-section. The study shows that rectangular flaps perform best in wave energy extraction. In the dual OWSC configuration, a decline in device performance is observed when the space between the two flaps equals one wavelength.

In identifying the concept to develop OWSC, a comprehensive understanding of the hydrodynamic aspects is required. As shown in Table 1, the literature related to OWSC device development in each scope is comprehensively described. Based on the literature study results, the concept of design and comprehensive analysis should not be discussed in detail. On the other hand, the parameter of the flap dimension plays a crucial role in ascertaining the efficacy of the OWSC device in harnessing energy from ocean waves. Therefore, this study focuses on three-dimensional hydrodynamics on OWSC technology through an alternative approach (numerical) followed by a validity process to maintain data actualization. Design investigation of the flap geometry is developed to investigate the optimal flap dimension parameters to improve device performance.

Table 1. Research gap of OWSC studies.

Study	Geometry	PTO System	Single Configuration	Dual Configuration
(Yu et al., 2014)	X	X	✓	✓
(Liu et al., 2022)	X	✓	✓	X
(Cui, Chen and Dai, 2023)	✓	X	X	✓
(Munoz, Huang and Thomas, 2024)	X	X	X	✓
Current study	✓	X	✓	X

Testing involves different wave period variations to obtain a comprehensive and in-depth analysis. In addition, the performance efficiency of the OWSC is reviewed based on the power generated from the device in the time domain model.

2. METHODOLOGY

2.1. Geometry

Oscillating wave surge converter (OWSC) is one of the WEC technologies developed by utilizing the direct impact of ocean waves to extract wave energy into mechanical energy (Cheng et al., 2020). As shown in Figure 1, this device utilizes a flap or plate hinged on the seabed as an oscillating body. A flap is a device that acts as a wave energy harvester and converts energy into a mechanical motion response.

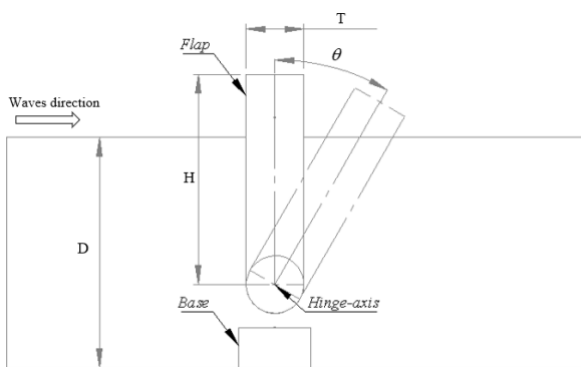


Figure 1. Schematic of oscillating wave surge converter (OWSC).

The research focuses on studying the OWSC scaling model to assess its hydrodynamic performance. The scaling model settings used in the flap dimensions refer to an experimental study conducted by Wei et al. (Wei et al., 2016). The mentioned study concentrated solely on the impact of slamming and viscosity effects on the

device's characteristics, resulting in a lack of available data regarding overall device performance.

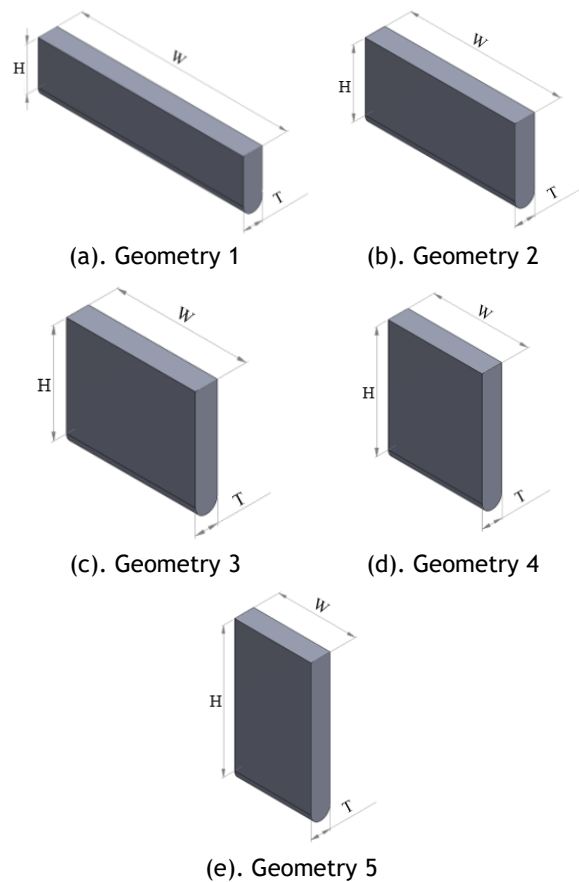


Figure 2. Geometric flap variations.

Table 2. Design parameters on geometric flap variations.

No	Dimensions (m)			Water depth (m)	Mass (Kg)
	H	W	T		
1	0.2	0.949			
2	0.3	0.665			
3	0.4	0.512	0.0875	0.305	4.27
4	0.5	0.416			
5	0.6	0.351			

In addition, investigation of device dimension parameters is carried out to investigate the size ratio that can show effective and efficient energy extraction performance. Figure 2 and Table 2 present variations in the flap model along with details of the dimension parameters.

2.2. Boundary Element Method

In the research scope, the boundary element method (BEM) is commonly used as a computational tool to model accurately the phenomena associated with the interaction of oceanic waves and Wave Energy Converter (WEC) technologies. BEM is introduced in this study through the linear potential flow theory by assuming incompressible, inviscid, and irrotational flow fluids (Julian *et al.*, 2024). As formulated in Equation (1), this theory is applied to calculate the wave force. This study introduces two different testing schemes: frequency domain and time domain. Equation (2) is the governing Equation used to calculate the hydrodynamic parameters that occur in the flap structure unit, including wave excitation force, mass matrix, added mass matrix, damping matrix, stiffness matrix, and motion response. In the time domain scheme, the flap structure response is calculated in mechanical device system units by calculating Nonlinear Hydrostatic and Froude-Krylov wave forces. The time domain scheme is set in Equation (3), which calculates the response structure periodically with constant amplitude (Lin and Pei, 2022).

$$\nabla^2 \phi(x, y, z, t) = \phi_I(x, y, z, t) + \phi_D(x, y, z, t) + \phi_R(x, y, z, t) = a_w \varphi(x, y, z) e^{-i\omega t} \quad (1)$$

$$\left[-\omega^2 (M_s + M_a(\omega)) - i\omega C(\omega) + K \right] X(\omega) = F(\omega) \quad (2)$$

$$M\ddot{X}(t) + C\dot{X}(t) + KX(t) + C_h\dot{X}(t) = F(t) \quad (3)$$

where:

- ϕ_I = Wave velocity potential
- ϕ_D = Wave diffraction potential

- ϕ_R = Wave radiation potential
- M_s = Mass matrix
- M_a = Added mass matrix
- C = Damping matrix
- K = Stiffness matrix
- X = Motion response
- F = Wave exciting force

2.3. Meshing and Boundary Condition

In this study, meshing is performed on the flap of the OWSC device as a discrete model to support numerical calculations. As in Figure 3, the 3D flap model is depicted as a surface domain so that the quadrilateral mesh can be utilized to divide the domain into smaller segments.

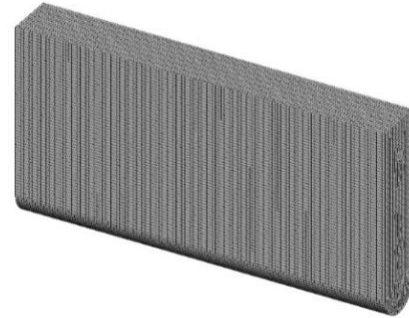


Figure 3. Detail of mesh.

In addition, the boundary conditions are defined to describe the approach to the actual phenomenon of the interaction of ocean waves with structures. In the process of modeling ocean waves, this study utilizes Airy Wave Theory, which is set out in Equation (4) (Newman, 2018).

Table 3. Ocean wave parameters.

No	Parameters		
	Amplitude (m)	Period (s)	Wavelength (m)
1	0.1	1.1	1.581
2	0.1	1.3	1.975
3	0.1	1.5	2.357
4	0.1	1.7	2.730
5	0.1	1.9	3.098
6	0.1	2.1	3.462
7	0.1	2.3	3.823
8	0.1	2.5	4.181
9	0.1	2.7	4.538
10	0.1	2.9	4.893

Modeling is carried out in the form of constant amplitude regular waves with the intermediate waves category ($1/20 < D/\lambda < 1/2$) followed by variations in wave periods to support the testing of hydrodynamic characteristics and performance on the OWSC device. Specifically, the variation in wave periods is described in Table 3.

$$\eta(x,t) = \frac{h}{2} \cos(\omega t - k(x \cos \theta)) \quad (4)$$

$$P_w = \frac{1}{2} \rho g A^2 C_g \quad (5)$$

$$C_g = \frac{1}{2} C_p \left\{ 1 + \frac{kD}{\sinh kD \times \cosh kD} \right\} \quad (6)$$

$$P_{OWSC} = |\tau(t) \times \omega(t)| \quad (7)$$

$$CWR = \frac{P_{OWSC}}{P_w \times Width} \quad (8)$$

where:

- η = Water surface elevation
- h = Wave high
- ω = Angular velocity
- k = Number of waves
- P_w = Waves power
- ρ = Density of fluid
- g = Gravity
- C_g = Group velocity
- C_p = Phase speed
- P_{OWSC} = OWSC power

Power data is used to measure the performance of OWSC devices, including units defined as the wave energy source and the energy absorption capability of the device. The power of the wave energy source is set in Equation (5), followed by the wave group velocity set in Equation (6). The performance of the OWSC device is defined in hydrodynamic power units calculated using Equation (7). The device's performance is described as the absolute value of the product between angular velocity and torque. In addition, the efficiency of the device is evaluated in capture width ratio (CWR) units set

in Equation (8) (Drew, Plummer and Sahinkaya, 2009; Ogden et al., 2022).

2.4. Mesh Independence Test

Numerical methodology employs a mesh independence test to ascertain the impact of the variation in the quantity of mesh elements on the sensitivity of alterations observed in the computed data. The study utilizes an independence test that is based on the method introduced by Roache (Roache, 1994).

$$RMS = \sqrt{\frac{1}{n} \sum_i x_i^2} \quad (9)$$

$$r = \frac{h_2}{h_1} \quad (10)$$

$$\bar{p} = \frac{\ln\left(\frac{f_3 - f_2}{f_2 - f_1}\right)}{\ln(r)} \quad (11)$$

$$GCI_{fine} = \frac{F_s |\epsilon|}{(r^{\bar{p}} - 1)} \quad (12)$$

$$GCI_{coarse} = \frac{F_s |\epsilon| r^{\bar{p}}}{(r^{\bar{p}} - 1)} \quad (13)$$

$$\epsilon = \frac{f_{n+1} - f_n}{f_n} \quad (14)$$

$$\frac{GCI_{coarse}}{GCI_{fine} r^{\bar{p}}} \approx 1 \quad (15)$$

$$f_{r_{h=0}} = f_1 + \frac{(f_1 - f_2)}{(r^{\bar{p}} - 1)} \quad (16)$$

where:

- RMS = Root mean square value
- r = grids ratio
- \bar{p} = Convergence order
- GCI = Grid convergence indec

Therefore, mesh variations are used based on the number of elements, including fine mesh (24930), medium mesh (12643), and coarse mesh (6308). Each number of mesh elements is set based on the grid refinement ratio set in Equation (10).

In the testing process, each mesh variation is calculated with the output data Root Means Square value of the motion response on the flap, specifically sea waves ($A = 0.1\text{m}$; $T = 1.7\text{s}$) set in Equation (9). The data obtained are samples for each mesh in the independence test. The order value is calculated through Equation (11). The Grid Convergence Index (GCI) supports the error value identification process, which is classified into two types: GCI_{fine} and GCI_{coarse}. Each component is calculated through Equations (12) and (13). The calculation results are tested through Equation (15) to ensure the actual value obtained is in accordance with the convergence zone. The calculation of the actual value is obtained through Equation (16) so that the error value of each mesh variation can be identified. The mesh independence test results show that the fine mesh category has the smallest error value. Therefore, this mesh type is determined as the computational setup in the data collection process. The mesh independence test results appear in Table 4 to provide more specificity.

Table 4. Mesh independence test results.

Mesh	Fine	Medium	Coarse
RMS	26.32610202	25.79957998	24.50960098
	1.292781749		
r	2		
GCI _{fine}	1.759%		
GCI _{coarse}	4.3103%		
$\frac{GCI_{coarse}}{GCI_{fine} r^p}$	1		
$f_{rh} = 0$	26.68922067		
Error	1.36054%	3.33333%	8.16667%

3. RESULTS AND DISCUSSION

3.1. Validation

After the verification (mesh independence test), validation is carried out to ensure the level of data actualization in accordance with the set limit standards. Validation involves comparing data obtained from a numerical approach with experimental data. In this study, the validation process was carried out by comparing experiments through secondary data in literature research conducted by Wei (Wei *et al.*, 2016).

The flap motion response variable compares data tested at certain waves ($A = 0.1$; $T = 1.9$). A comparison between the numerical results and the experimental data is illustrated in Figure 4. The results of the approach show that the numerical data has a relatively consistent level of similarity in the motion response in each time series test. Thus, the tendency of the comparison of numerical data to experiments shows valid results.

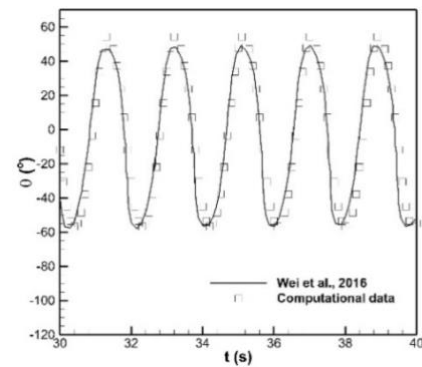


Figure 4. Validation result.

3.2. Analysis

This study investigates the characteristics and hydrodynamic performance of the OWSC device, followed by investigating the dimensions of the flap geometry. Figure 5 shows how the device responds to each geometry variation on specific input waves. It is observed that each variation of geometry parameters shows similar response characteristics, specifically the angular deviation due to periodic wave incidents. This phenomenon aligns with the findings of the study conducted by Li *et al.* (Li *et al.*, 2022), which indicates that the OWSC device exhibits periodic motion characteristics. However, significant geometry changes affect the maximum response of the device and the resulting angular phase. The computational results show that the highest maximum deviation is achieved in geometry variation 2.

This condition is achieved when the flap height resembles the water surface level and is almost symmetrical in each direction of deviation. Symmetric flap deviation response can also be achieved in geometry variation 1 condition, where the flap height is lower than the water surface level.

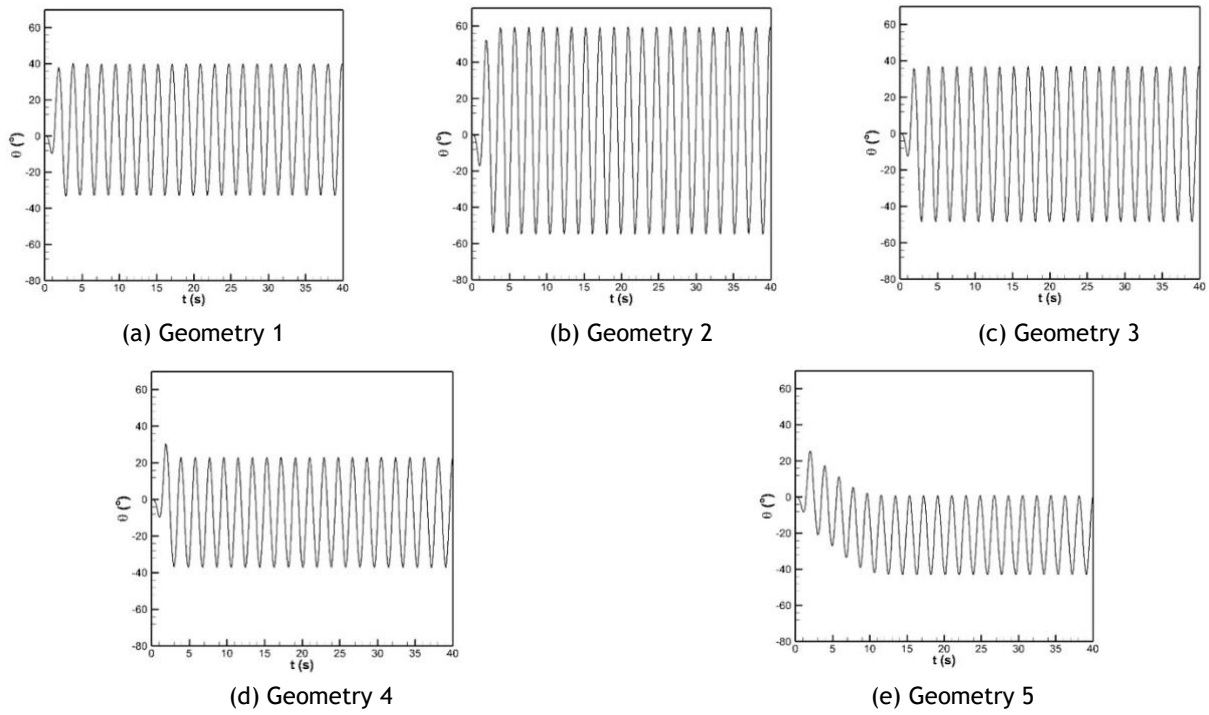


Figure 5. Motion response of flap on specific ocean waves ($A= 0.1m$; $T= 1.9s$)

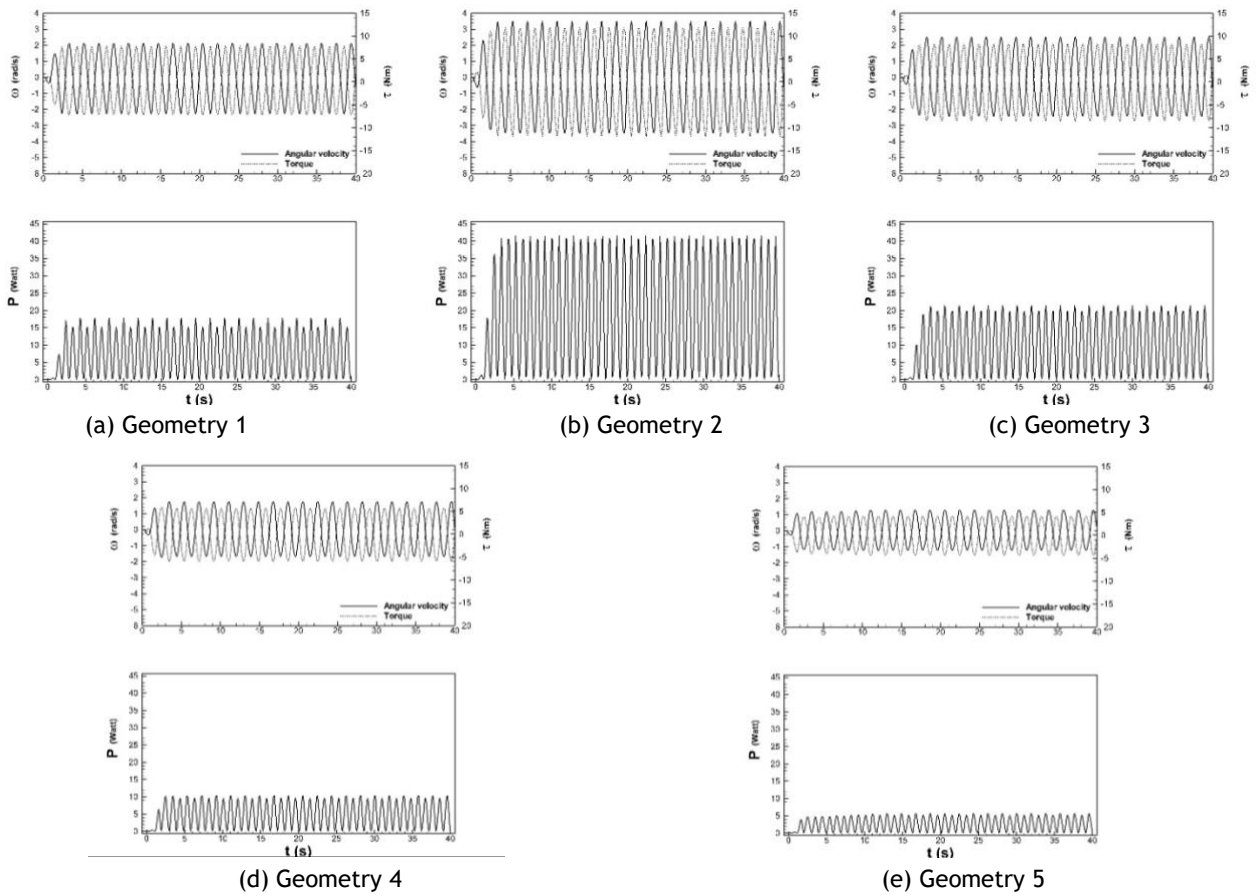


Figure 6. Hydrodynamic parameters; angular velocity (rad/s), torque (Nm), power (Watt).

On the other hand, the device response in geometry variations 3, 4, and 5 begins to shift in the maximum angle produced. The maximum deviation of the device is increasingly dominant in the negative direction. This condition is achieved because the flap geometry height is greater than the water surface level. In addition, there is a shift in the angular phase in the response, especially in flap geometry variations 4 and 5. The dynamics that affect the phenomena cause both variations to experience a delay in response to wave incidents.

In supporting the phenomenon of device response due to sea wave incidents, [Figure 6](#) shows to support the occurring dynamics that occur. Angular velocity, torque, and hydrodynamic power are displayed to investigate each characteristic of the geometry variation. Based on the test results, it can be identified that each variation of the geometry change in the flap affects the ability to absorb energy from wave impacts. The dynamic parameters presented reveal a trend of results that align with several earlier studies ([Wei et al., 2016](#)). However, there is a notable discrepancy in the amplitude of these parameters, particularly regarding the torque output generated. This observation is accompanied by assumptions about boundary conditions related to fluid properties, including the presumption of inviscid, irrotational, and incompressible flow. Although the flap variation has a constant mass, changes in shape can affect different inertia and force distributions. The width parameter (W) in the flap dimension plays a role in the flap's ability to absorb the amount of sea wave energy sources per area. In contrast, the height parameter (H) plays a role as a variable affecting energy transmission to the structure in torque units. In geometry variations 1 and 3, both have similar characteristics. This condition can be seen from the angular velocity and torque output produced.

From a geometric point of view, the dimensional parameters in the two variations show different shapes. Regarding width, geometry variation 1 has a more tremendous energy absorption potential. However, geometry 2 has a more significant flap height than geometry 1, so the compensation for energy absorption in

geometry 2 is more effective by utilizing greater torque. On the other hand, the energy absorption capability decreases in geometry variations 4 and 5. Despite having a higher flap dimension, considering the fixed water surface level, this parameter has no significant effect on the torque generated. From each variation of flap dimensions, geometry 2 shows the most optimal ratio comparison between dimensions. Although it does not have a larger width dimension than geometry 1, the torque output generated is more effective by utilizing the flap height that is equivalent to the wave elevation. This condition is directly proportional to the hydrodynamic power, where the peak value of the power generated at a specific wave period is able to reach 41.52 Watt. The geometry model underwent testing at specific wave period intervals to achieve a more thorough analysis. The test was conducted at wave specifications ($A=0.1\text{m}$; $T=1.1\text{-}2.9\text{s}$).

In [Figure 7](#), the maximum angular deviation, average angular velocity, and torque are shown as parameters representing the capability of each device to the variation of wave period. Several related studies utilize analysis in the wave period domain to provide a more in-depth analysis space for assessing the capabilities of OWSC devices at certain period intervals ([Lin and Pei, 2022](#); [Liu et al., 2022](#); [Munoz, Huang and Thomas, 2024](#)). From the maximum angular deviation data, the curve trend is classified into two groups: geometry 1 and 2 as the first trend group and geometry 3, 4, and 5 as the second trend group. In the first trend group, the relationship of the maximum angular deviation experienced by the flap is directly proportional to the increase in wave period.

However, this condition is limited to a specific period until the maximum angular deviation as a flap response decreases. Overall, the maximum deviation in geometry 2 is more significant than in geometry 1. Both variations show the peak point of the maximum deviation at period $T=1.5\text{ s}$, 61.09° , and 40.23° , respectively. On the other hand, the second trend group shows a different change in maximum angular deviation. In geometry variation 3, there is no significant change in deviation until the period reaches $T=1.5\text{s}$. In contrast, geometries 4 and 5 experience

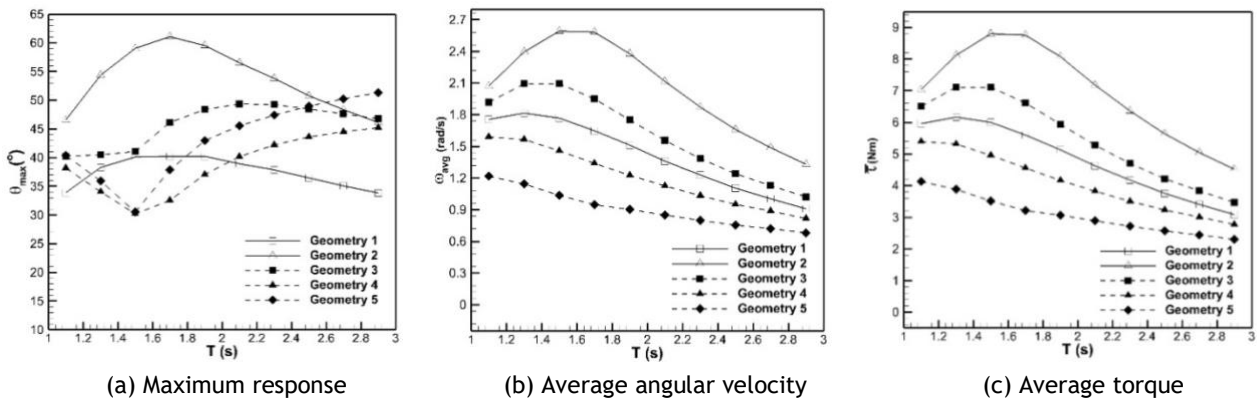


Figure 7. Hydrodynamic parameters in period domain; maximum response ($^{\circ}$), average angular velocity (rad/s), and average torque (Nm).

a decrease in the maximum angular deviation value. After the second trend group reaches the period $T > 1.5s$, the increase in maximum deviation occurs continuously except in geometry 3, where the peak point of maximum angular deviation reaches 49.33° at the wave period $T = 2.1s$.

On the other hand, the average angular velocity and torque output to changes in wave period have a similar trend at each point. It is evident that Geometry 2 exerts the most substantial influence on each variable under consideration, where the maximum value is achieved at period $T = 1.5s$ with an average angular velocity of 2.59 rad / s and torque of 8.8 Nm . The influence of waves on the dynamics of other geometry variations decreased at each period. In geometry variations 1 and 3, hydrodynamic parameters that contribute significantly occur in geometry 3 despite a similar character shown in the deviation response. More specifically, the hydrodynamic parameters obtained are processed as power output. This activity aims to examine the hydrodynamic performance of the device at each wave period.

Figure 8 shows that the contribution of hydrodynamic parameters working on each device variation is directly proportional to the power output produced. Statistically, the most optimum device performance was found in geometry variation 2, where the maximum power was achieved up to 22.81 Watts at wave period $T = 1.5s$. In addition, followed by geometry 3, geometry 1, geometry 4, and geometry 5, each of

which has an average maximum power of 14.88 Watts , 11.18 Watts , 8.52 Watts , and 5.02 Watts .

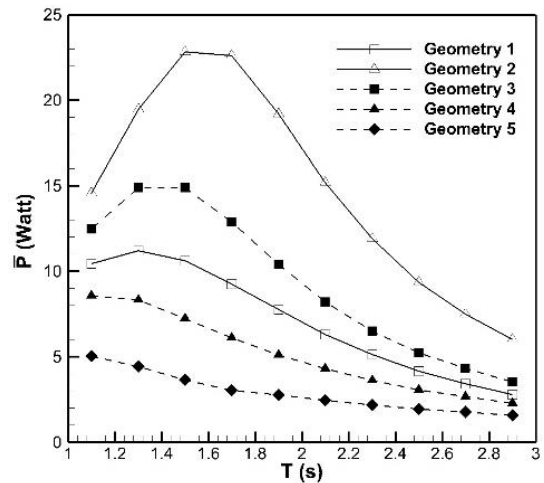


Figure 8. Hydrodynamic performances of OWSC; Average power output (Watt).

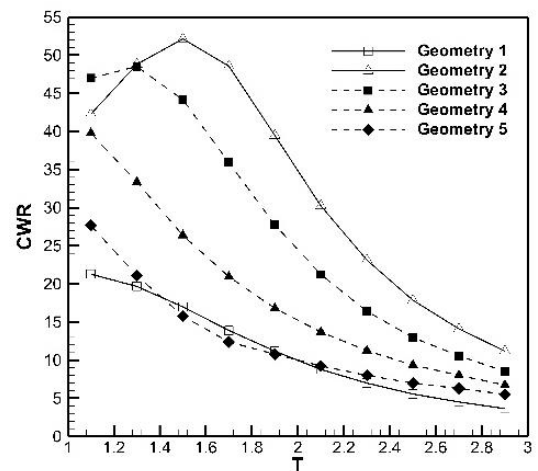


Figure 9. Hydrodynamic efficiency of OWSC; CWR (%).

In addition, the capability of each device is reviewed from the efficiency (CWR) perspective. As shown in Figure 9, at the beginning of the period, the maximum efficiency is achieved by geometry variation 3, which is 46.9%. In contrast, geometries 1, 2, 4, and 5 achieve efficiencies of up to 21.28%, 42.28%, 39.77%, and 27.67%, respectively. Although geometry variation 1 has the most extensive W dimension parameter, the resulting efficiency performance is unsatisfactory. As the wave period changes, the trend of maximum efficiency changes, where overall geometry 2 dominates the highest efficiency level. The condition where the maximum efficiency occurs reaches 52.14% at wave period $T = 1.5s$. In addition, geometry two shows capability with a broader period interval. Thus, the investigation process of the OWSC device is achieved by deciding geometry variation 2 as the best performance of flap dimension parameter. This finding indicates that the OWSC device's maximum efficiency aligns well with its operational mechanism's specifications. Previous research suggests that the efficiency of the OWSC device is typically estimated to be in the range of 50%-70% (Babarit *et al.*, 2012). This study contributes to the field by optimizing the design parameters of the flap geometry, which is an important factor influencing the performance of OWSC technology. As a result, this finding paves the way for further advancements in OWSC technology by exploring various contributing factors.

4. CONCLUSION

This research concentrates on numerical testing of the characteristics and hydrodynamic performance of the Oscillating Wave Surge Converter device. Followed by variations in flap dimension parameters, the study also concentrates on investigating device parameters that show the best geometry ratios. Based on the computational results, identification of flap geometry design on the OWSC device significantly affects the characteristics and performance of the device in exploiting ocean wave energy. From a geometric perspective, the dimensional parameters in the two variations exhibit distinct

shapes. In terms of width, geometry variation 1 demonstrates a greater potential for energy absorption.

However, geometry 2 features a taller flap compared to geometry 1, allowing for more effective compensation of energy absorption through the utilization of greater torque. Conversely, the energy absorption capabilities are diminished in geometry variations 4 and 5. Even though these variations possess larger flap dimensions, the fixed water surface level renders this parameter relatively ineffective in influencing the torque generated. Flap geometry variation 2 is investigated as the most optimal dimension parameter. This condition is achieved ideally by the proportion of the appropriate flap width, followed by the flap height parallel to the elevation of the ocean waves.

In addition, the performance of geometry 2 is supported by hydrodynamic parameters, including angular velocity and torque, that dominate significantly in each variation of the wave period. This phenomenon is directly proportional to the hydrodynamic power output, which reaches a maximum value of up to 41.52 Watts with a CWR efficiency achievement of 52.14%.

REFERENCES

- Babarit, A. *et al.* (2012) 'Numerical Benchmarking Study Of A Selection Of Wave Energy Converters', *Renewable Energy*, 41, pp. 44-63. Available at: <https://doi.org/10.1016/j.renene.2011.10.002>.
- Cheng, Y. *et al.* (2020) 'Fully Nonlinear Investigations On Performance Of An OWSC (Oscillating Wave Surge Converter) In 3D (Three-Dimensional) Open Water', *Energy*, 210, p. 118526. Available at: <https://doi.org/10.1016/j.energy.2020.118526>.
- Cui, J., Chen, X. and Dai, S. (2023) 'Numerical Study On Dual Oscillating Wave Surge Converter With Different Cross-Section Shapes Using SPH Under Regular Waves', *Ocean Engineering*, 271, p. 113755. Available at: <https://doi.org/10.1016/j.oceaneng.2023.113755>.
- Drew, B., Plummer, A.R. and Sahinkaya, M.N. (2009) 'A Review Of Wave Energy Converter Technology', *Proceedings of the Institution of Mechanical Engineers, Part A: Journal of Power and Energy*, 223(8), pp. 887-902. Available at: <https://doi.org/10.1243/09576509JPE782>.

- Haitao, Z. (2012) *Hydrodynamic Research of a Bottom-Hinged Flap Wave Energy Convertor*. PhD Thesis. Zhejiang University.
- Julian, J. et al. (2024) 'Study Of Hydrodynamic Characteristics In Oscillating Wave Surge Converter', *Jurnal Polimesin*, 22(2), pp. 158-164. Available at: <https://doi.org/10.30811/jpl.v22i2.4715>.
- Junejo, F., Saeed, A. and Hameed, S. (2018) '5.19 Energy Management in Ocean Energy Systems', in I. Dincer (ed.) *Comprehensive Energy Systems*. Oxford: Elsevier, pp. 778-807. Available at: <https://doi.org/10.1016/B978-0-12-809597-3.00539-3>.
- Kadu, A.V., Rathod, V. and Matre, V. (2019) 'A Review on Seed Sowing Method and Alternative Method for Small Farmers', *International Journal of Research in Engineering, Science and Management*, 2(7), pp. 194-196.
- Khaligh, A. and Onar, O.C. (2017) *Energy Harvesting: Solar, Wind, and Ocean Energy Conversion Systems*. CRC Press. [Print].
- Li, M. et al. (2022) 'State-Of-The-Art Review Of The Flexibility And Feasibility Of Emerging Offshore And Coastal Ocean Energy Technologies In East And Southeast Asia', *Renewable and Sustainable Energy Reviews*, 162, p. 112404. Available at: <https://doi.org/10.1016/j.rser.2022.112404>.
- Lin, Y. and Pei, F. (2022) 'Numerical Study On Bottom-Hinged Plate Wave Energy Converter Geometry Design', *Ocean Engineering*, 260, p. 112050. Available at: <https://doi.org/10.1016/j.oceaneng.2022.112050>
- Liu, Y. et al. (2022) 'Performance Enhancement Of A Bottom-Hinged Oscillating Wave Surge Converter Via Resonant Adjustment', *Renewable Energy*, 201, pp. 624-635. Available at: <https://doi.org/10.1016/j.renene.2022.10.130>.
- Liu, Z. and Zhang, G. (2024) 'Overtopping Performance Of A Multi-Level CROWN Wave Energy Convertor: A Numerical Study', *Energy*, 294, p. 130795. Available at: <https://doi.org/10.1016/j.energy.2024.130795>.
- Munoz, D.B., Huang, L. and Thomas, G. (2024) 'Optimal Array Arrangement Of Oscillating Wave Surge Converters: An Analysis Based On Three Devices', *Renewable Energy*, 222, p. 119825. Available at: <https://doi.org/10.1016/j.renene.2023.119825>.
- Newman, J.N. (2018) *Marine Hydrodynamics, 40th anniversary edition*. MIT Press. [Print].
- O'Boyle, L. et al. (2015) 'The Value of Full Scale Prototype Data - Testing Oyster 800 at EMEC, Orkney', in *Proceedings of the 11th European Wave and Tidal Energy Conference. 11th European Wave & Tidal Energy Conference*, Nantes, France: European Wave & Tidal Energy (EWTEC) (The European Wave and Tidal Energy Conference), pp. 1-10.
- Ogden, D. et al. (2022) 'Review Of WEC-Sim Development And Applications', *International Marine Energy Journal*, 5(3), pp. 293-303. Available at: <https://doi.org/10.36688/imej.5.293-303>.
- Roache, P.J. (1994) 'Perspective: A Method for Uniform Reporting of Grid Refinement Studies', *Journal of Fluids Engineering*, 116(3), pp. 405-413. Available at: <https://doi.org/10.1115/1.2910291>.
- Sugianto, D.N. et al. (2017) 'Wave Energy Reviews in Indonesia', *International Journal of Mechanical Engineering and Technology (IJMET)*, 8(10), pp. 448-459.
- Wei, Y. et al. (2016) 'Wave interaction with an Oscillating Wave Surge Converter. Part II: Slamming', *Ocean Engineering*, 113, pp. 319-334. Available at: <https://doi.org/10.1016/j.oceaneng.2015.12.041>
- Yu, Y.-H. et al. (2014) 'Design and Analysis for a Floating Oscillating Surge Wave Energy Converter', in *ASME 2014 33rd International Conference on Ocean, Offshore and Arctic Engineering*, American Society of Mechanical Engineers Digital Collection. Available at: <https://doi.org/10.1115/OMAE2014-24511>.
- Zhang, D. et al. (2013) 'Wave Energy Converter Of Inverse Pendulum With Double Action Power Take Off', *Proceedings of the Institution of Mechanical Engineers, Part C: Journal of Mechanical Engineering Science*, 227(11), pp. 2416-2427. Available at: <https://doi.org/10.1177/0954406213475760>.

